Available online at www.sciencedirect.com
SCIENCE DIRECT®
International Journal of Heat and Mass Transfer 47 (2004) 4315–4325
International Journal of HEAT and MASS TRANSFER
www.elsevier.com/locate/ijhmt

Determination of the Soret coefficient of magnetic particles in a ferrofluid from the steady and unsteady part of the separation curve

Th. Völker [a,*], E. Blums [b], S. Odenbach [a]

[a] ZARM, University of Bremen, Am Fallturm, D-28359 Bremen, Germany
[b] Institute of Physics, University of Latvia, Salaspils, Germany

Received 31 July 2003; received in revised form 23 April 2004

Abstract

Experiments on the particle separation in a vertical thermodiffusion column are used to investigate the separation (Soret effect) in ferrofluids. The use of a two-sectional column with internal walls of low thermal capacity allows analyzing the initial part of the unsteady separation curves as well as the steady state regime. The Soret coefficient calculated from the measurements of the separation dynamics agrees well with the one found from the steady separation limit reached in long-time experiments especially if the solutal buoyancy is low.

1. Introduction

Suspensions of magnetic nanoparticles—commonly called magnetic fluids or ferrofluids—show normal liquid behavior coupled with superparamagnetic properties. This enables a magnetic control of their flow and other physical characteristics by means of magnetic fields with a strength of about 50 mT. The magnetic particles, having a mean diameter of about 10 nm, are usually made of magnetite (Fe_3O_4). They are covered with a surfactant made from long chained organic molecules, prohibiting agglomeration due to van der Waals attraction. Since magnetic agglomeration and sedimentation of the particles are prevented by thermal energy, stable suspensions can be produced. The volume concentration of the magnetic component is usually about 2–10 vol.% and various carrier liquids like oils, kerosene or water can be used. (For information on magnetic fluids see e.g. Refs. [1–3].)

Thermodiffusion (also called: Ludwig–Soret effect or thermal diffusion) is a composite effect in which an external temperature gradient leads to a concentration gradient of one fraction in a fluid mixture. This effect is of fundamental importance in classical physics [4] but is also likely to have important consequences for natural systems especially underground reservoirs of multicomponent fluids (oil and salty aquifers) which are subject to significant thermal gradients [5].

Thermodiffusion is observed in many molecular systems, for example in gas and liquid mixtures and in solutions of salts and metals see e.g. Refs. [6–8]. As a general rule, the Soret coefficient is very small for these systems ($10^{-5}\ K^{-1} \leqslant S_T \leqslant 10^{-2}\ K^{-1}$). In contrast the role of thermodiffusion in disperse systems (colloids and suspensions) can be significant. Here the Soret coefficient may be two to four orders of magnitude higher than the typical values for known molecular systems.

From a technical point of view the Soret effect may play a significant role in the problem of long term stability of ferrofluids. If temperature gradients are present, i.e. when the fluid is used as a heat transport medium, the thermophoretic transfer of particles will affect the stability of the ferrofluid strongly.

* Corresponding author. Tel.: +49-421-218-4790; fax: +49-421-218-2521.
E-mail address: voelker@zarm.uni-bremen.de (Th. Völker).

0017-9310/$ - see front matter © 2004 Elsevier Ltd. All rights reserved.
doi:10.1016/j.ijheatmasstransfer.2004.05.019

Nomenclature

a	half-width of the channel
d	particle diameter
c	volume fraction of particles
D	mass diffusion coefficient of particles ($= k_B T/6\pi\eta d$)
Gr_T	thermal Grashof number ($= \beta_T g \Delta T a^3/\nu^2$)
Gr_c	concentrational Grashof number ($= \beta_c g c_0 a^3/\nu^2$)
g	gravitational acceleration
j_x	mass flux along coordinate x
k	Soret number ($= S_T \Delta T$)
k_B	Boltzmann's constant
L	height of the channel
L_e	effective height of the chambers (see (2))
p	parameter of Laplace transformation
R	non-dimensional vertical concentration gradient (see (5))
S_T	Soret coefficient
S	parameter of the Soret convection ($= kGr_c/Gr_T$)
Sc	Schmidt number ($= \nu/D$)
$T(\pm a)$	cold and hot wall temperature
ΔT	temperature difference ($= T(a) - T(-a)$)
t	time
u	vertical convection velocity, non-dimensional (see (5)
u_z	vertical convection velocity
$\tilde{x}$	coordinate across the channel
x	coordinate across the channel, non-dimensional (see (5))
z	vertical coordinate (oriented opposite to g)

Greek symbols

β_T, β_c	thermal ($\beta_T = -\frac{1}{\rho 0}\frac{\partial \rho}{\partial T}$) and solutal ($\beta_c = \frac{1}{\rho 0}\frac{\partial \rho}{\partial c}$) expansion coefficient
η	dynamic viscosity of the colloid
ν	kinematic viscosity of the colloid ($= \eta/\rho$)
ρ	mass density of the colloid
σ	non-dimensional concentration (see (5))
τ	non-dimensional time (see (5))

It is very difficult to perform direct measurements of the Soret effect in ferrofluids using conventional optical methods. Holographic interferometry which has been successfully used to examine high gradient magnetic separation (HGMS) processes in colloids under isothermal conditions [9] cannot be employed to measure the Soret coefficient since a temperature gradient is present. More preferable are indirect measurements such as the use of thermodiffusion columns discussed here. The advantage of this technique is the possibility to measure the particle separation dynamics during the separation process with high accuracy until the steady state is reached. The aim of this study is the question how strong a ferrofluid can be separated under the influence of a temperature gradient.

2. Analytical model and separation characteristics

2.1. Formulation of the problem

Classical thermodiffusion theories include several very strong simplifications. In particular, a steady concentration profile $c(x)$ across the channel (a thin gap between two flat vertical walls $\tilde{x} = \pm a$ of a height $L \gg a$) is assumed. In addition, the vertical convection velocity $v_z = u_z(x,t)$ is only determined by the thermal buoyancy force. The mass transfer problem is usually written in a simplified form as unsteady one-dimensional diffusion of the mean concentration of the solute across the channel [10,11]

$$\frac{\partial \bar{c}}{\partial t} = D_k \frac{\partial^2 \bar{c}}{\partial z^2} + u_T \frac{\partial \bar{c}}{\partial z} \tag{1}$$

where $D_k = D(1 + 64/9! \cdot (Gr_T Sc)^2)$ denotes the "convective diffusion" coefficient, $k = S_T \Delta T$ is called the Soret parameter and $u_T = 4/6! \cdot DkGr_T Sc/a$ is the convective separation parameter. As boundary conditions a conservation of the solute's mass in two connected chambers at the channel ends ($z = 0$ and $z = L$) is used:

$$\left.\frac{dc}{dt}\right|_{z=0,L} = \mp \frac{j_z}{L_e}. \tag{2}$$

Here j_z is the mean vertical particle flux in the channel ends, $L_e = V_e/S_e$ represents the ratio of the volume of the chambers at the column ends V_e to the sectional area of the channel S_e.

The solution of Eq. (1) with the boundary conditions (2) predicts a linear growth of the vertical concentration gradient with time during the initial separation process but such a law is usually not observed in ferrofluid experiments [12–14]. The reason for this discrepancy bases on the fact that the diffusion coefficient of solutes in colloids is very low compared with molecular systems. For a typical value of $D \approx 10^{-12}$ m^2/s for ferrite nanoparticles in magnetic fluids the time, which is necessary to reach a steady concentration profile across a channel with $a \approx 0.5$ mm (a typical value for thermodiffusion columns), exceeds one hour. Besides, due to a great difference between the densities of the particles and the carrier liquid, the thermodiffusive transfer causes strong solute buoyancy which acts additional to the thermal

one. The corresponding changes in the vertical convection intensity influence the separation process significantly. This so-called "forgotten effect" [15] should be taken into account when the heat and mass transfer in the column is analyzed. The initial part of the separation curves taking the combined action of thermal and solutal buoyancy into account has been analyzed in [16–19].

Here simplified analytical models which allow the analysis of the full separation curve including the asymptotic region of saturation are presented. The mass transfer in a thermodiffusion column consisting of a flat vertical channel with $a \ll L$ and of identical top ($z = L$) and bottom ($z = 0$) separation chambers is considered using the one dimensional quasi-steady Boussinesq equation for the convection velocity

$$\rho\nu\frac{\partial^2 u_z}{\partial\tilde{x}^2} - (\rho - \rho_0)g = 0, \tag{3}$$

under the assumption that the density of the fluid depends only on the temperature and the particle concentration $\rho = \rho_0 - \beta_T(T - T_0) + \beta_c(c - c_0)$ with the thermal expansion coefficient $\beta_T = -\frac{1}{\rho_0}\frac{\partial\rho}{\partial T}$ and the concentration expansion coefficient $\beta_c = -\frac{1}{\rho_0}\frac{\partial\rho}{\partial c}$.

Due to the low convection velocity the inertia forces are neglected and thus the unsteady linearized two-dimensional mass transfer equation for the particle concentration with $c \ll 1$ as usual for ferrofluids becomes

$$\frac{\partial c}{\partial t} + u_z\frac{\partial c}{\partial z} = D\frac{\partial^2 c}{\partial\tilde{x}^2} + S_T D\frac{\partial}{\partial\tilde{x}}\left(c\frac{\partial T}{\partial\tilde{x}}\right). \tag{4}$$

In the vertical direction the convective mass transfer significantly exceeds the corresponding diffusive ones. Therefore terms containing the second derivative on the vertical coordinate z have been neglected on the right side of (4). The thermal relaxation time of the channel does not exceed several seconds for usual values of $a < 1$ mm. Therefore the distribution of the temperature across the channel is assumed to be constant $T - T_0 = \Delta T\tilde{x}/(2a)$ with $\Delta T = T(a) - T(-a)$. The boundary conditions for the concentration are the non-permeability of the channel walls $j_x(\pm a) = 0$ and the mass conservation in the channel ends which can be written in the form (2).

Introducing non-dimensional parameters

$$\begin{aligned} R &= \frac{\beta_c g a^4}{\nu D}\frac{\partial c}{\partial z}, \quad \vartheta = \frac{2(T - T_0)}{\beta_T\Delta T}, \\ \sigma &= \frac{2(c - c_0)\beta_c}{\beta_T\Delta T}, \quad u = \frac{2u_z\nu}{\beta_T g a^2\Delta T}, \\ \tau &= \frac{Dt}{a^2} \quad \text{and} \quad x = \frac{x'}{a}, \end{aligned} \tag{5}$$

and using the steady concentration profile $\sigma = x$ Eqs. (3) and (4) become the non-dimensional form

$$\frac{\partial^2 u}{\partial x^2} + x - \sigma = 0, \quad \frac{\partial\sigma}{\partial\tau} + Ru = \frac{\partial^2\sigma}{\partial x^2} + \frac{k}{2}\frac{\partial\sigma}{\partial x}. \tag{6}$$

The corresponding boundary conditions are

$$\begin{aligned} \sigma'(\pm 1) + \frac{k}{2}\sigma(\pm 1) = -S \quad \text{and} \quad \frac{\partial\bar{\sigma}}{\partial\tau}_{|z=0,L} \\ = \mp\frac{a}{4L_c}Gr_T Sc\int_{-1}^{+1} u\sigma\,\mathrm{d}x. \end{aligned} \tag{7}$$

Here the parameter $S = KGr_c/Gr_T$ represents the ratio of the solute buoyancy to the thermal one.

2.2. General trend of the separation curves

In general, the vertical concentration gradient R depends on the spatial position and on the time. Such a dependence as well as the complicated form of the boundary condition (7) does not allow to obtain a precise solution of the given integro-differential problem. Only an approximate analysis of various asymptotic mass transfer regimes can be performed. Considering molecular liquids with small Soret coefficients, the terms with k in the second equation (6) and in the first boundary condition (7) are usually omitted. In Ref. [19] it is shown that this simplification, independently of the value of S, can be used as long as the Soret parameter k does not exceed the value $k \approx 2$. Thermodiffusion experiments in magnetic fluids with typical values of $S_T \approx 0.1\ \mathrm{K}^{-1}$ [13] are usually within this interval of k. In such a case the steady concentration profile is linear, $\sigma = -Sx$. Such linearity is valid also for the steady vertical gradient of concentration R_∞ [11] since the non-dimensional parameter of convective separation $u_T a/D_k$ in Eq. (1) usually does not exceed the above-mentioned limit 2. Here we assume that for small separation parameters the gradient $R = R(\tau)$ does not depend on the vertical coordinate z during the whole separation process. In such an approximation the second boundary condition (7) can be rewritten in the form

$$\frac{\partial R}{\partial\tau} = \frac{1}{2}\left(Gr_T Sc\frac{a}{L}\right)^2\frac{L}{L_c}\int_{-1}^{+1} u\sigma\,\mathrm{d}x. \tag{8}$$

Qualitative insight in the specifics of the separation dynamics can be obtained by an analysis of Eqs. (6) using a Laplace transformation in time. For simplicity the transformation of the convective term in the mass transfer equation does not account for a time-dependence of the velocity. This means that the analysis can be considered to be correct only for liquids with sufficiently small values of the separation parameter S.

The approximate Laplace transformation ($\tau \to P$) mentioned above allows to obtain simple concentration and velocity profiles:

$$u = A_1 \sinh(k_1 x) + A_2 \sinh(k_2 x) - \frac{p}{R} x \tag{9}$$

$$\sigma = A_1 k_1^2 \sinh(k_1 x) + A_2 k_1^2 \sinh(k_2 x) + x \tag{10}$$

with

$$A_1 = \frac{1}{Q_1}\left[(1+S)\sinh(k_2) + \frac{p}{R} k_2^3 \cosh(k_2)\right], \tag{11}$$

$$A_2 = \frac{1}{Q_1}\left[(1+S)\sinh(k_1) + \frac{p}{R} k_1^3 \cosh(k_1)\right], \tag{12}$$

$$Q_1 = k_2^3 \cosh(k_2)\sinh(k_1) - k_1^3 \cosh(k_1)\sinh(k_2) \tag{13}$$

and

$$k_{1,2} = \sqrt{\frac{p}{2} \pm \sqrt{\left(\frac{p^2}{4} + R\right)}} \tag{14}$$

The solution of the integral equation (8) with these profiles leads to a transcendent equation of complex arguments which allows to determine the dependence $R = R(p, S)$. Unfortunately, it is not possible to realize a reverse transformation and to represent the results in a form of analytical dependence R as a function of real time. Nevertheless, it is possible to analyze a general trend of the separation process. Fig. 1 shows a set of dynamic separation curves for fluids of various $Gr_T Sc$ and S as a function of the parameter $1/p$. The curves refer to several characteristic regimes. In the initial stage

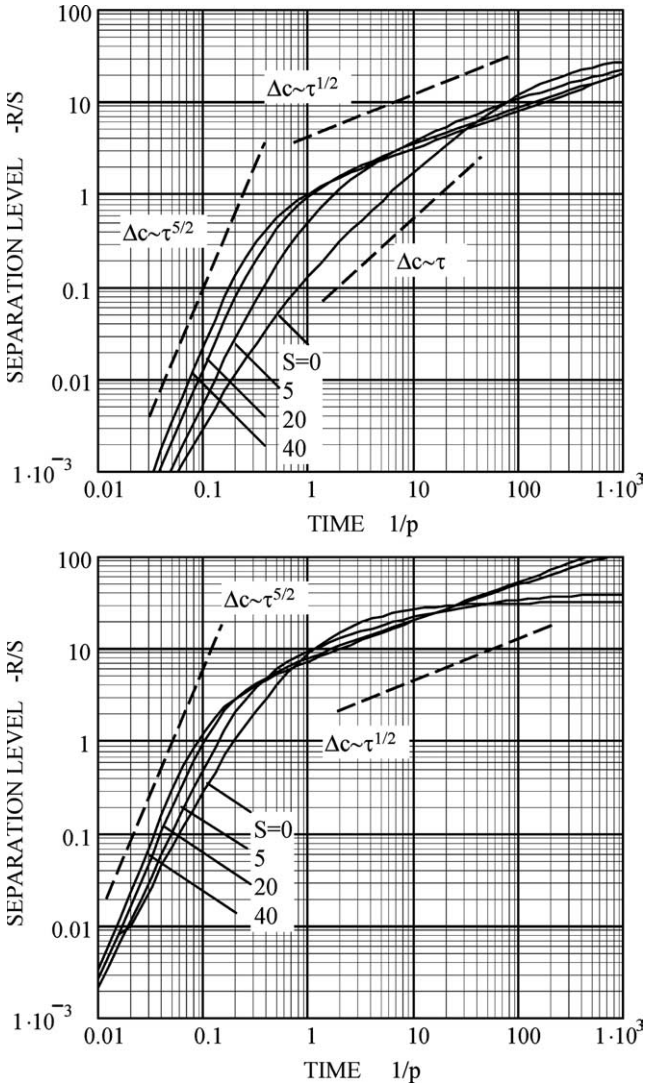

Fig. 1. Dynamics of particle separation for $Gr_T Sca/(L_c L)^{0.5} = 4$ (upper figure) and $Gr_T Sca/(L_c L)^{0.5} = 40$ (lower figure).

the curves for all S follow to the "5/2" law $R \sim \tau^{5/2}$. This part reflects the unsteadiness of the vertical mass flux during the formation of concentration profile across the channel [14,17]. As smaller the Soret coefficient and lower the solute buoyancy, as sooner sets in the linear regime $R \sim \tau$. This regime corresponds to a steady concentration profile across the channel in columns of low convection intensity [19]. At high thermal Rayleigh and Soret numbers the linear part of the separation curves cannot be observed. The separation process in the column starts to saturate before the concentration profile c reaches a steady state. For $S > 1$, the concentration difference in the channel ends develops in accordance with the "square-root" law $R \sim \tau^{0.5}$ observed in experiments [14]. For $S > 10$ the slope of the separation curves in the asymptotic regime $-R/S > 10$ is even lower, $\Delta\sigma \sim \tau^{0.4}$. Besides, if $S \gg 1$, the relaxation time for reaching the steady separation state as well as the final difference of particle concentration in the channel ends increases significantly.

2.3. Unsteady separation within $R \ll 1$

Considering the initial part of the separation process within $R \ll 1$, the convective term in the mass transfer equation (6) may be neglected and the unsteady concentration and quasi-steady velocity profiles can be calculated analytically. Employing the above mentioned simplification for small k values, we obtain

$$u = \frac{1}{6}(1+S)(x-x^3) + 2S\sum_{n=1}^{\infty}\frac{[x+(-1)^n\sin\alpha_n x]}{\alpha_n^4}\mathrm{e}^{-\alpha_n^2\tau}, \tag{15}$$

$$\sigma = -S\left(x + 2\sum_{n=1}^{\infty}\frac{(-1)^n\sin\alpha_n x}{\alpha_n^2}\mathrm{e}^{-\alpha_n^2\tau}\right) \text{ with}$$

$$\alpha_n = (2n-1)\frac{\pi}{2}. \tag{16}$$

Fig. 2 represents the non-dimensional unsteady vertical mass flux j_z (integral of the right side of (8) accounting for profiles (15) and (16)). During the formation of the concentration profile across the channel ($\tau < 0.02$), the mass flux follows a characteristic dependence $j_z \sim \tau^{3/2}$—independently of the value of S—which corresponds to the "5/2" law for R shown in Fig. 1. Reaching approximately $\tau \approx 1$, the stabilization process completes, the steady flux strongly depends on the parameter S. At positive Soret coefficients the particles are collected in the bottom end of the channel, the increase of the parameter S causes an intensification of the convective mass transfer. For negative Soret coefficients and in the interval $0 > S > -1$ for the separation parameter the

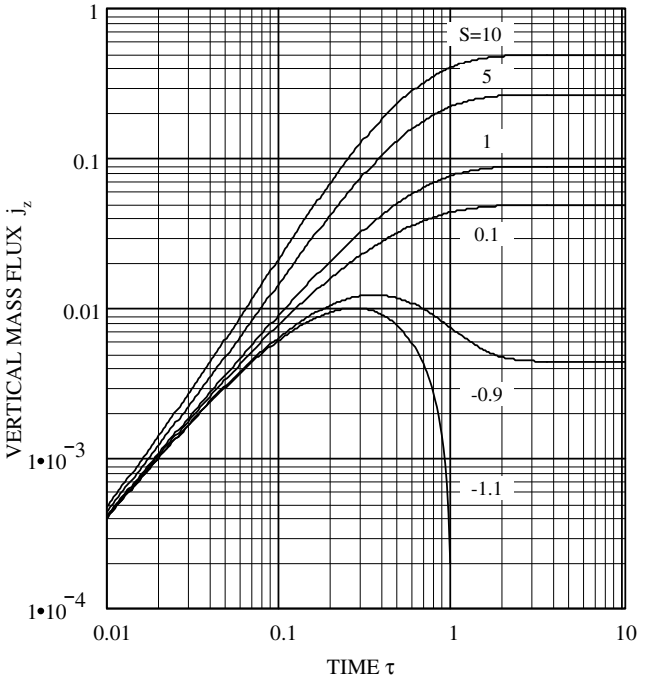

Fig. 2. Unsteady vertical mass flux during formation of the concentration profile across the channel calculated accounting for the velocity and concentration and profiles (15) and (16) respectively.

particles are transferred to the upper channel end. The solute buoyancy now suppresses the thermal convection. Therefore, the intensity of vertical mass transfer is less than that for positive S. If $S < -1$, a collection of particles in the top of the column can be observed only in a short initial interval of time. Reaching a certain time τ_s, the solute buoyancy in the channel starts to prevail; both the velocity profile and the vertical mass flux change their direction. Obviously, during the transition period develop convective instabilities which destroy the one-dimensional shear flow in the channel and the separation dynamics cannot be analyzed in the frame of the approximate model concerned here.

The initial part of the separation process with the "3/2 law" for the mass flux shown in Fig. 2 corresponds to a regime, for which a boundary layer concept is valid for the concentration profile [17,18]. Resolving Eqs. (6) in the frame of this boundary layer approximation and introducing the corresponding profiles in (8), we obtain the following simple expression for the concentration difference in the channel ends [19]:

$$-\frac{R}{S} = \frac{8}{45\sqrt{\pi}}\left(Gr_T Sc\frac{a}{L}\right)^2 \frac{L}{L_c}\tau^{2.5}\left[1 - \frac{15\sqrt{\pi}}{16}\tau^{0.5} + \frac{6}{7}\tau + S\left(\frac{3}{7}\tau - \frac{15\sqrt{\pi}}{64}\tau^{1.5}\right)\right]. \quad (17)$$

In the region $\tau < 0.1$ this dependence agrees as well with the calculated results presented in Fig. 1 as with those performed using the profiles (15) and (16). Thus, the expression (17) can be used to calculate the Soret coefficient from the measured separation curves.

2.4. Asymptotic steady separation level

Within the limit $p \to 0$ the formulas (9) and (10) describe the stabilized quasi-steady regime of the convection and concentration profiles in the channel. From (8) we obtain the following equation of the vertical mass transfer:

$$\frac{\partial R}{\partial \tau} = \frac{L}{L_c}\left(Gr_T Sc\frac{a}{L}\right)^2 \frac{1}{4\gamma^4}\left[(1+S)\left(\frac{4P_2}{\gamma P_1} - 2\right) + (1+S)^2\left(\frac{P_2}{\gamma P_1} - \frac{P_3}{P_1^2}\right)\right] \quad (18)$$

with the coefficients $\gamma = R^{1/4}$, $P_1 = \sinh\gamma\cos\gamma + \sin\gamma\cosh\gamma$, $P_2 = \sinh\gamma\sin\gamma$ and $P_3 = \sin^2\gamma + \sinh^2\gamma$. Considering small vertical concentration gradients $/R/ \ll 1$ from (18) we obtain a linear dependence

$$\frac{R}{S} = -\frac{(1+S)}{90}\frac{L}{L_c}\left(Gr_T Sc\frac{a}{L}\right)^2 \tau, \quad (19)$$

which for $S \to 0$ coincides well with the one found in the conventional thermodiffusion column theories. This follows from the solution of Eq. (1) for $\tau \ll 1$ and it is seen graphically in Fig. 1a for small values of S and $Gr_T Sc$. Expression (19) is valid for $S > -1$. Negative stratification ($R > 0$) of particles in the column at $S < -1$ is impossible due to the reason discussed above.

Introducing $\partial R/\partial\tau = 0$ in (18) we obtain a transcendent equation for the calculation of the asymptotic steady concentration difference in the column ends as a function of the parameter S

$$S + 1 = \frac{2P_1(\gamma P_1 - 2P_2)}{P_1 P_2 - \gamma P_3} \quad (20)$$

Fig. 3 represents the dependence $R_\infty(S)$ graphically ($Rn = -R_\infty$). For small $S \ll 1$, Rn is given by the relation $Rn = 63S/2$ known from theories considering a pure thermal convection in the channel (see, for example, Ref. [10]). From the presented curve (the formulas allow to obtain results also for negative Soret coefficients until $S > -4.8$ but, of course, a physical meaning have only those results which correspond to positive S), it follows that the solute buoyancy causes a significant increase of the steady concentration difference in the channel ends. Nevertheless, considering the separation at high values of S, we should remember that the presented analytical model assumes a linearity of the vertical concentration gradient which cannot be guaranteed for high values of the separation parameter. The maximal concentration difference in a column with equal channel ends cannot exceed the value $\Delta c/c_0 = 2$ which is equal to $Rn = 2Gr_T Sc$. The upper level of the separation parameter, at which the presented simplified analytical model is valid, can be found by a comparison with the results of a numerical simulation of the mass transfer equation accounting for $R = R(z)$. In the present work we will make some conclusions on the basis of long time separation measurements by comparing the values of

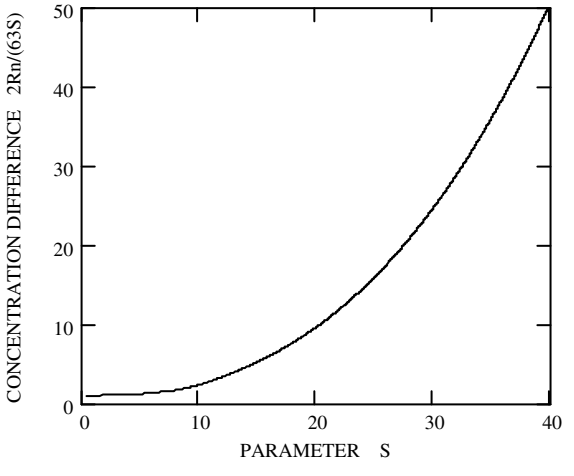

Fig. 3. The influence of solute buoyancy on the steady concentration difference in the channel ends (dependence (18) at $\partial R/\partial\tau = 0$).

Soret coefficients obtained from the initial part of the separation curves (formula (17)) with those calculated from the steady concentration difference using (18) for the asymptotic regime $\partial R/\partial\tau = 0$.

3. Experimental setup and procedure

3.1. The thermodiffusion column

As mentioned before there are only two analytical models (17) and (20) which can be used to evaluate the Soret coefficient from the experimentally found data, so it is necessary to measure the initial regime as well as the steady concentration difference with high precision to allow a quantitative comparison of theory and experiment.

The initial part is characterized by extremely small concentration changes whereas the steady part cannot be reached in an ordinary experimental time. Therefore we have developed two identical thermodiffusion columns to investigate both time regimes separately.

Each column (see Fig. 4) consists of two parallel vertical flat channels with a small gap of width $2a = 0.5$ mm and two connected separation chambers. The two channel technique has been designed to increase the measurable effect especially in the initial part of the separation process. The column is made from plastic which has low heat conductivity and low thermal expansion. The hot and cold walls are made from brass with polished inner surfaces [20].

The determination of particle concentration in the ferrofluid is carried out by means of inductance changes in sensor coils [21]. To enable in-situ measurement the sensor coils are mounted inside the separation chambers.

To avoid interaction between the two independent but equal fluid flows in both gaps, the chambers are divided in two parts. Due to the fact that the output signal is very small and that small temperature changes can influence the measurement results, temperature controllers are mounted in both chambers and at the heated and cooled walls. Particle concentration measurement in the two chambers is determined by measuring the resonance frequency of an LC oscillator. Therefore the coils inside the two chambers are connected with two independent oscillators. The inductance of the coils increases linearly with volume concentration of magnetic particles leading to a decrease of the resonance frequency of the connected oscillator. This frequency change is converted to a DC-output signal for a faster detection in a multimeter. The concentration in the chambers can be determined twice a second with an accuracy of 10^{-6} vol.% which is three orders of magnitude more than in previous experiments [21].

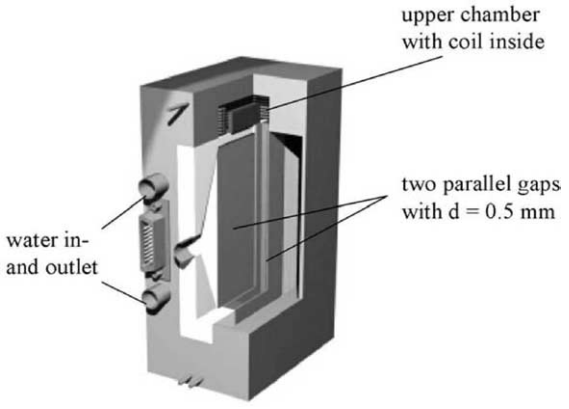

Fig. 4. Principal sketch of the thermodiffusion column.

3.2. The ferrofluid sample

Experiments are performed with a kerosene based ferrofluid containing magnetite particles. The mean particle diameter $d = 9$ nm with a small size distribution is calculated by magnetogranulometry from magnetization curves [22]. The surfactant is oleic acid, thus the thickness of the protection layer is approximately 2 nm. The original fluid has a volume concentration of magnetic particles of $c_0 = 0.078$. A dilution series was made up to 0.007. The viscosity of each fluid was measured by means of capillary viscosimeters. With this information one can calculate the Brownian diffusion coefficient D_0 as it is shown in Table 1.

3.3. The experimental procedure

As mentioned above it has been the scope of this work to test the two analytical models for the initial as well as the stationary part of the separation curve and to compare the resulting Soret coefficients from both parts. For the measurement of the volume concentration of the magnetic particles in the both chambers one needs on the one hand a high accuracy of the resulting impedance signal and on the other hand a precise calibration to define all parameters like magnetic field or temperature influencing the concentration measurement system. For example the flow discharging into the chamber leads to a change of the temperature distribution which affects the determination of the particle concentration seriously. To control such effects, calibration measurements have been performed with the carrier liquid.

Because of the short time interval in which the model for the initial part is valid the determination of the starting point is of great importance. A few hours before the measurement starts the gap walls are held at mean temperature T_0. At $t = 0$ the outer walls of the channels are cooled down to T_1 whereas the two inner walls are heated up to T_2. The relaxation time to reach

Table 1
Characteristic numbers of the diffusion process for constant $\Delta T = 10$ K

c [vol.%]	v [10^{-6} m^2/s]	D_0 [10^{-11} m^2/s]	Gr_T	Gr_c
7.8	5.1	4.3	0.37	14.71
6.00	4.1	3.4	0.58	17.51
4.0	3.0	2.5	1.09	21.80
2.5	2.6	2.2	1.45	18.13
2.0	2.4	2.0	1.70	17.03
1.5	2.2	1.8	2.03	15.20
0.7	2.0	1.7	2.45	8.58

approximately 95% of the working temperature difference is less than 10 s.

For the long term measurements the whole setup has to be stable for a couple of months. This includes not only the concentration measurement but also the tempering system. Thus the setup was placed into a self-sufficient room for the measurement period with constant temperature conditions.

To evaluate the Soret coefficient from both parts of the separation curve a ferrofluid with low volume concentration of magnetic particles $c_0 = 0.02$ was used to ensure the validity of the assumption of negligibility of particle interaction in both models.

To test the theoretical predictions described in Section 2.4 the temperature difference was varied from 5 to 20 K to determine the influence of the driving force on the separation dynamics as well as on the steady state limit. A second set of experiments has been performed with a dilution series starting from an original ferrofluid with $c_0 = 0.078$ to obtain information about the influence of particle–particle interaction on the separation process. The first mentioned changes correspond to a constant value of the separation parameter, while the second set is equivalent to a variation of S.

4. Experimental results and discussion

4.1. Determination of the Soret coefficient from the unsteady separation part

A first series of experiments has been performed to test the theoretical predictions made for the initial interval of time of the separation process. Fig. 5 shows the initial part of the separation curve as observed for $\Delta T = 10$ K ($T_1 = 20$ °C, $T_2 = 30$ °C, $T_0 = 25$ °C). The concentration difference is positive, that means that the Soret coefficient is also positive, the direction of thermodiffusive transport is toward decreasing temperature. The plotted lines are the curves from the analytical theory (see formula (17)) for different values of the Soret coefficient. The measured separation curve shows the $\Delta c/c_0 \sim t^{2.5}$ behavior for times $t \leqslant 200$ s. The small difference to the calculated curves reflects not only the measurement error but also the uncertainty of D_0. Expressions used for its calculation base on the assumption of monodispersity of particles and negligibility of particle interaction. The comparison between calculated and experimentally found curves gives a value for the Soret coefficient of $S_T = +0.15 \pm 0.02$ K^{-1}. The same value was also found in other ferrofluid samples containing the same amount of magnetic particles but different carrier liquids [13,19]. It was shown there, that the $\Delta c/c_0 \sim t^{2.5}$ behavior scales linear with the viscosity as the theoretical model described in Section 2.2 predicts.

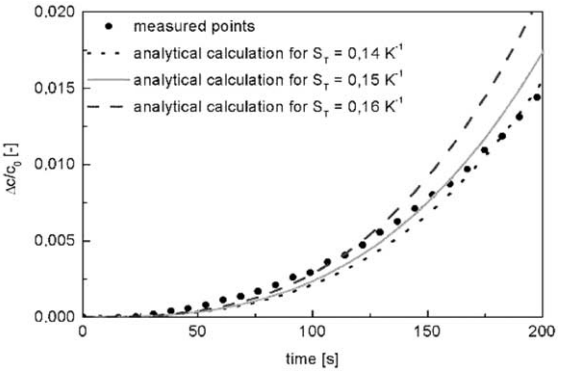

Fig. 5. The initial part of the separation process measured at $\Delta T = 10$ K with a fluid with $c_0 = 0.02$ together with theoretical fits for different Soret coefficients.

In another group of experiments the influence of the volume fraction of magnetic nanoparticles on the Soret coefficient has been studied. Therefore a dilution series was made from a ferrofluid with $c_0 = 7.8$ vol.% whereas the fluid with $c = 2$ vol.% is equal to the fluid discussed above.

It was found that the Soret coefficient decreases with increasing volume concentration of particles as will be seen later in Section 4.2 (see Fig. 9). There the open circles represent the experimental data found from the initial part of the separation process. As one can see at the highest dilution ($c = 0.005$) the Soret coefficient was determined to be $S_T = 0.2$ K^{-1}, whereas it is $S_T = 0.05$ K^{-1} at $c = 0.078$. This leads to the conclusion that the

increase of particle density in a ferrofluid leads to a significant hindrance of their mobility.

4.2. Determination of the Soret coefficient from the asymptotic steady separation level

Fig. 6 shows the long term development of the separation process measured using the sample with the highest dilution ($c = 0.02$) at various ΔT. As seen from the figure, a separation level of $\Delta c/c_0 \approx 1.72$ is reached in all experiments independent from the temperature difference. Following the theoretical calculations shown in Fig. 3 this leads to a Soret coefficient of $S_T = +0.14$ K^{-1} which is practically identical with the value found from the unsteady part of the separation curve. This leads to the conclusion that for diluted colloids both models, the one for the unsteady and the one for the steady state part, allow the determination of the Soret coefficient of magnetic nanoparticles in a ferrofluid.

It is interesting to note that the separation level reached in the long term experiments is independent from the driving temperature difference. This is also found in the theoretical model since the concentration difference shown in Fig. 3 depends on the parameter S only, which does not depend on the temperature difference

$$s = k\frac{Gr_c}{Gr_T} = S_T c_0 \frac{\beta_c}{\beta_T}.$$

For the fluid used in these experiments, having $c_0 = 0.02$, the value of S can be determined to be $S = 15$ since the ratio β_c/β_T is usually 5×10^3 K^{-1} for ferrofluids and the Soret coefficient was determined to $S_T = 0.15$ K^{-1}.

Besides the constant steady separation level a dependence on the time to reach this level on the driving temperature is seen in Fig. 6. Starting with a temperature difference of 20 K between the walls it takes 27 days to separate the ferrofluid. The time increases with decreasing temperature, i.e. decreasing driving force, leading to 102 days for $\Delta T = 5$ K. This change of the time to reach the steady separation level is also predicted in the theoretical model (see Fig. 1) but due to the Laplace transformation there is no information about the real time.

In the experiments the thermal Grashof number increases linear with increasing temperature difference, starting with $Gr_T = 1.25$ at $\Delta T = 5$ K and ending with $Gr_T = 5$ at $\Delta T = 20$ K. The Schmidt number is kept constant at $Sc = 10^5$. From (17) it follows that in the initial regime of the separation process the unsteady concentration difference should be proportional to the product $Gr_T Sc$. From the results presented in Fig. 1 it can be seen, that also the time to reach the saturation level decreases with an increase of ΔT. Unfortunately, the real time for reaching the steady separation level cannot be obtained from the curves presented in Fig. 1. Thus a time law can only be found from the experimental data plotting the time needed to reach the steady state as a function of the driving force ΔT. The experimentally found $t \sim 1/\Delta T$ law is shown in Fig. 7.

Finally Fig. 8 gives the results of the second set of experiments mentioned in Section 3.3. In these experiments, which were performed at constant difference of the driving temperature $\Delta T = 10$ K, fluids of various particle concentration have been used. Thus, the solute buoyancy has been varied, while the thermal driving force is kept constant. Now the behavior of the separation curves is quite different. The concentration influences both, the dynamical part of separation curves as well as the saturation value of the concentration difference. Theory predicts that an increase in solutal buoyancy at constant Soret coefficient should cause an increase of the steady separation level. The observed

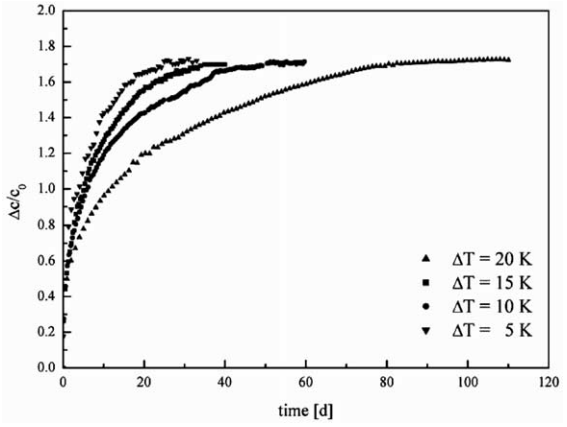

Fig. 6. The steady state part of the separation process for the same fluid ($c_0 = 0.02$) as in Fig. 5 for different driving temperature differences.

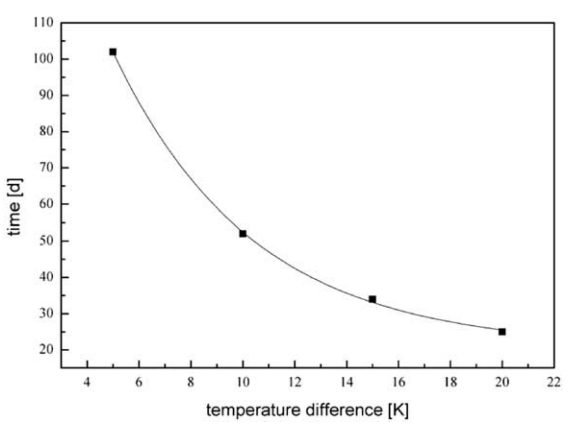

Fig. 7. The influence of the driving temperature difference on the time to reach the steady state of the separation process (solid line is a fit to the eye).

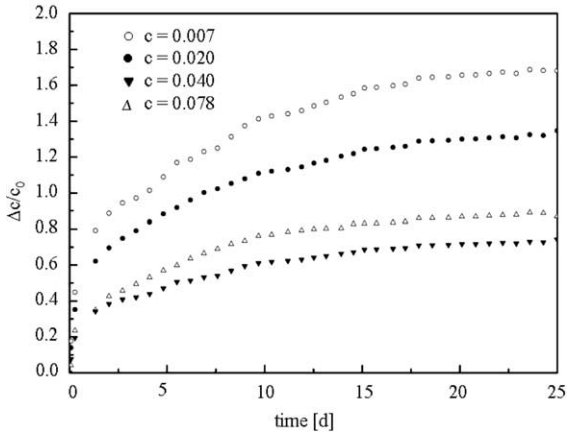

Fig. 8. The influence of the particle's volume fraction on the separation dynamics measured using a dilution series of ferrofluids ranging from $c_0 = 0.078$ to $c_0 = 0.02$.

reduction of the asymptotic values of Δc (Fig. 8) for fluids with increasing c_0 reflects a reduction of the Soret coefficient appearing with the increase of the particle concentration as mentioned in Section 4.1. The values of the Soret coefficient calculated from the measured steady concentration difference with the account of the theoretical dependence (20), which is graphically shown in Fig. 3, are given in Fig. 9 together with the results obtained from the initial unsteady part of separation curves. As it was already mentioned above, for the strongly diluted fluid with $c_0 = 0.02$ both values agree very well. In fluids of higher c_0 the values of the Soret coefficient which are found from the steady separation level, are slightly less than those calculated from the unsteady separation curves, but still within the margin of error. Such a discrepancy is principally expected since the theory is developed considering a linearity of the vertical mean concentration gradient R. According to

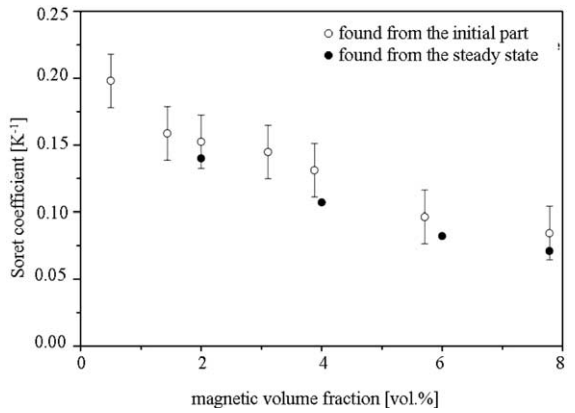

Fig. 9. The dependence of the Soret coefficient on the particle volume fraction.

Ref. [11] such an approximation is valid until the parameter $u_T L/D_k$ in Eq. (1) does not exceed 0.3. This value correspond to a separation level approximately equal to $\Delta c/c_0 < 1$. In our experiments the steady concentration difference exceeds this level; therefore, calculations based on the linear approximation (8) reach their limit of validity.

5. Conclusions

A theoretical model which describes the separation process in magnetic fluids in thermodiffusion columns has been developed. This model allows the determination of the Soret coefficient in the unsteady regime of the separation process as well as in the steady state using experimentally found separation curves.

The Soret coefficient was measured for surfacted nanoparticles in a ferrofluid with a particle volume concentration $c = 0.02$ to be $S_T = 0.15\ K^{-1}$. The measurement was performed by means of a special thermodiffusion column. This value for S_T was found from the initial part of the thermodiffusion process as well as from the steady state regime. Thus both theoretical models described here are experimentally approved for diluted colloids.

As further test of the theory experiments with a variation of the driving temperature difference ΔT showed a constant steady separation level and a variation of the time span needed to separate the fluid. Both results are also in accordance with the theoretical prediction. Finally it could be shown, that an increase of the volume concentration of magnetic particles yields a decrease of the Soret coefficient due to particle–particle interaction reducing the mobility of the particles. This reduction is so pronounced, that it yields a reduction of the steady separation limit in the long term experiments.

In case of high thermal and solutal Grashof numbers the theoretical approach for the steady separation regime could principally be improved taking into account the non-homogeneity of the vertical particle concentration gradient.

References

[1] R.E. Rosensweig, Ferrohydrodynamics, Cambridge University Press, Cambridge, 1985.
[2] E. Blums, A. Cebers, M.M. Maiorov, Magnetic fluids, Walter de Gryuter, Berlin, New York, 1997.
[3] S. Odenbach, Magnetoviscous effects in ferrofluids, LNPm71, Springer Verlag, 2002.
[4] W. Deen, Analysis of Transport Phenomena, Oxford University Press, Oxford, 1998.
[5] L. Kempers, A comprehensive theory of the Soret effect in a multicomponent mixture, in: Proceedings of the IMT4, Bayreuth, 2000.

[6] W. Köhler, Thermodiffusion in polymer solutions as observed by forced Rayleigh scattering, J. Chem. Phys. 98 (1) (1993).
[7] T. Alboussiere et al., Convective effects in the measurement of diffusivities and thermotransport coefficients of liquid metal alloys and the use of magnetic field, Entropie 218 (1999).
[8] B. Brinkmann, Entwicklung einer Messapparatur zur holographischen Untersuchung der Thermodiffusion in korrosiven Fluessigkeiten unter Verwendung der Finite-Element-Methode, Dissertation, TH Aachen.
[9] E. Blums, A.Yu. Chukrov, A. Rimsa, Some problems of submicron particle transfer near the filter element of high gradient magnetic separation, Int. J. Heat Mass Transfer 30 (1987) 1607–1613.
[10] G.D. Rabinowich, R.J. Gurevich, G.I. Bobrova, Thermodiffusion Separation in Liquid Dispersions, Nauka i Tehnika, Minsk, 1971 (Chapter 1) (in Russian).
[11] E. Blums, G. Kronkalns, R. Ozols, The characteristics of mass transfer processes in magnetic fluids, J. Magn. Magn. Mater. 39 (1983) 142–146.
[12] A. Mezulis, E. Blums, G. Kronkalns, M.M. Maiorov, Measurements of thermodiffusion of nanoparticles in magnetic colloids, Latvian J. Phys. Tech. Sci. (5) (1995) 37–50.
[13] E. Blums, A. Mezulis, M.M. Maiorov, G. Kronkalns, Thermal diffusion of magnetic nanoparticles in ferrocolloids: experiments on particle separation in vertical columns, J. Magn. Magn. Mater. 169 (1997) 220–228.
[14] E. Blums, S. Odenbach, A. Mezulis, M.M. Maiorov, Soret coefficient of nanoparticles in ferrofluids in the presence of a magnetic field, Phys. Fluids 10 (1998) 2155–2163.
[15] O. Ecenarro, J.A. Madariaga, J. Navarro, C.M. Santamaria, J.A. Carrion, J.M. Saviron, Non-steady density effects in liquid thermal diffusion columns, J. Phys.: Condens. Mater. 1 (1989) 9741–9746.
[16] T. Voelker, E. Blums, S. Odenbach, Thermodiffusive processes in ferrofluids, Magnetohydrodynamics 37 (2001) 274–278.
[17] E. Blums, A. Mezulis, Thermal diffusion and particle separation in ferrocolloids, in: A. Alemany, Ph. Marty, J.R. Thibault (Eds.), Transfer Phenomena in Magnetohydrodynamic and Electroconducting Flows, Kluwer Academic, Dortrecht, Boston, London, 1999, pp. 1–16.
[18] E. Blums, S. Odenbach, Thermophoretic separation of ultrafine particles in ferrofluids in thermal diffusion column under the effect of a MHD convection, Int. J. Heat Mass Transfer 43 (2000) 1637–1649.
[19] E. Blums, S. Odenbach, Dynamics of thermodiffusive separation of ferrocolloids in vertical columns: the effect of solute buoyancy, Magnetohydrodynamics 37 (2001) 187–194.
[20] Th. Völker, Thermodiffusion in Ferrofluiden, Dissertation, Universitat Bremen, 2002.
[21] S. Odenbach, Forced diffusion in magnetic fluids under the influence of a strong magnetic field gradient, Z. Phys. B 94 (1994) 331–335.
[22] M.M. Maiorov, private communication.